AAPS PharmSciTech, Vol. 12, No. 4, December 2011 (© 2011)
DOI: 10.1208/s12249-011-9716-9

Research Article

Preparation, Statistical Optimization, and *In vitro* Characterization of Insulin Nanoparticles Composed of Quaternized Aromatic Derivatives of Chitosan

Reza Mahjub,[1,5] Farid Abedin Dorkoosh,[1] Mohsen Amini,[2,7] Mohammad Reza Khoshayand,[3,8] and Morteza Rafiee-Tehrani[1,4,6,9]

Received 18 August 2011; accepted 6 October 2011; published online 27 October 2011

Abstract. The aim of this study was the preparation, optimization, and *in vitro* characterization of insulin nanoparticles composed of methylated *N*-(4-*N*,*N*-dimethylaminobenzyl), methylated *N*-(4-pyridinyl), and methylated *N*-(benzyl) chitosan. Three types of derivatives were synthesized by the Schiff base reaction followed by quaternization. Nanoparticles were prepared by the polyelectrolyte complexation method. Experimental design D-optimal response surface methodology was used for the optimization of the nanoparticles. Independent variables were pH of polymer solution, concentration ratio of polymer/insulin, and also polymer type. Dependent variables include size, zeta potential, polydispersity index (PdI), and entrapment efficiency (EE%). Optimized nanoparticles were studied morphologically by transmission electron microscopy (TEM), and *in vitro* release of insulin from nanoparticles were determined under phosphate buffer (pH=6.8) condition. Although a quadratic model has been chosen to fit the responses for size, PdI, and EE%, the zeta potential of the particles has been best fitted to 2-FI model. The optimized nanoparticles were characterized. The size of the particles were found to be 346, 318, and 289 nm; zeta potentials were 28.5, 27.7, and 22.2 mV; PdI of particles were 0.305, 0.333, and 0.437; and calculated EE% were 70.3%, 84.5%, and 69.2%, for methylated (aminobenzyl), methylated (pyridinyl), and methylated (benzyl) chitosan nanoparticles, respectively. TEM images show separated and non-aggregated nanoparticles with sub-spherical shapes and smooth surfaces. An *in vitro* release study of the prepared nanoparticles showed that the cumulative percentage of insulin released from the nanoparticles were 47.1%, 38%, and 68.7% for (aminobenzyl), (pyridinyl), and (benzyl) chitosan, respectively, within 300 min.

KEY WORDS: D-optimal response surface experimental design methodology; insulin nanoparticles; methylated *N*-(4-*N*,*N*-dimethylaminobenzyl) chitosan; methylated *N*-(4-pyridinyl) chitosan; methylated *N*-(benzyl) chitosan.

INTRODUCTION

Various systems have been used for drug delivery and targeting. Among them, liposomes, microparticles, and nanoparticles have been extensively studied (1). Formulation of liposomes requires complicated techniques and specialized equipments that may be unavailable globally (2). On the other hand, the instability of liposomes in different environments has been proven (3). Microparticulate drug delivery systems have overcome many of difficulties encountered with liposomes (*e.g.*, complication of production and also instability of particles), but the large size of microparticles may increase the possibility of opsonization by macrophages and may also decrease the paracellular permeability. Therefore, nanoparticles as small and stable carriers can be a good candidate for drug delivery purposes (4–7).

Based on the facts mentioned above, various nanostructures including fullerenes, quantum dots, dendrimers, magnetic nanoparticles, and polymeric nanoparticles have been developed and extensively studied in biological applications (8,9). Polymeric nanoparticles have been extensively studied for peptide and protein delivery (10–12).

Entrapment of peptides and proteins to mucoadhesive polymeric nanoparticles is regarded as the best approach for prevention of drug instability against degradation in gastrointestinal (GI) and also promotion and prolongation of peptide permeability across intestinal epithelium. Therefore, these nanocarriers can be a good candidate for oral delivery

[1] Department of Pharmaceutics, Faculty of Pharmacy, Tehran University of Medical Sciences, Tehran, Iran.
[2] Department of Medicinal Chemistry, Faculty of Pharmacy, Tehran University of Medical Sciences, Tehran, Iran.
[3] Department of Food and Drug Control and Pharmaceutical Quality Assurance Research Center, Faculty of Pharmacy, Tehran University of Medical Sciences, Tehran, Iran.
[4] Nanotechnology Research Center, Faculty of Pharmacy, Tehran University of Medical Sciences, Tehran, Iran.
[5] School of Pharmacy, Hamedan University of Medical Sciences, Hamedan, Iran.
[6] School of Pharmacy, Tehran University of Medical Sciences, P.O. Box 14395/459, Tehran 14, Iran.
[7] Drug Design and Development Research Center, Tehran University of Medical Sciences, Tehran, Iran.
[8] Correspondence for statistical experimental design section Department of Food and Drug Control and Pharmaceutical Quality Assurance Research Center, Faculty of Pharmacy, Tehran University of Medical Sciences, Tehran, Iran.
[9] To whom correspondence should be addressed. (e-mail: rafitehr@ams.ac.ir)

of proteins and peptides. Chitosan is a mucoadhesive biodegradable and biocompatible polymer which can be used in pharmaceutical industry as dissolution enhancer, absorption enhancer, and sustained release agent in oral drug formulation (13). Mucoadhesive properties of the polymer, can justify the use of chitosan as paracellular permeability enhancer in formulation of hydrophilic macromolecular drugs. Mucoadhesiveness of chitosan is reported to be the result of ionic interaction between positively charged amino group in chitosan and negatively charged functional groups in surface of epithelial cells (14).

The major disadvantage of chitosan is that it is a weak base with apparent pK_a of 5.5, therefore, in acidic pH, the primary amino functional groups that present in the backbone structure are protonated and positively charged but in neutral and alkaline environments, these amino groups lose their charge and the polymer become insoluble in such medium (15). Considering the fact that only the protonated portion of chitosan can pose permeation enhancement properties, it can be concluded that in intestine where the pH of environment is above the apparent pK_a of the polymer, application of chitosan in drug formulation has little effect on increase in paracellular permeability of hydrophilic macromolecules (16). In order to overcome this problem, several chitosan derivatives including alkylated chitosan (17–19), thiolated chitosan (20), pegylated chitosan (21), and so on have been synthesized. Among them quaternized alkylated chitosan derivatives such as trimethyl chitosan (TMC) have been extensively studied (22,23). These alkylated derivatives can pose permanent positive charge in wide pH range and makes the polymer soluble in different regions of GI tract. Recently, aromatic derivatives of chitosan have attracted the interest of researchers. Rojanarata *et al*. (24) have reported the synthesis and characterization of methylated chitosan containing an aromatic ring called methylated *N*-(4-*N*,*N*-dimethylaminobenzyl) chitosan. It has been shown that this derivative of chitosan can be used as effective gene carriers and pose greater transfection efficiency compared with chitosan and TMC. It has also been demonstrated that due to the amphiphilic nature of the cell membrane, quaternized derivatives of chitosan that contain aromatic ring as hydrophobic residue can enhance the cellular absorption of macromolecules across Caco-2 cell monolayer in free soluble form via enhancement of the interaction between the cell membrane and the polymer (25,26). On the other hand, formulation of macromolecules as nanoparticulate drug delivery systems has more effectiveness over formulation with free soluble polymers as the absorption enhancer. Nanoparticles can easily infiltrate into the mucus layer and deliver the macromolecules to the site of absorption and also improve the stability of macromolecules (27). Therefore, by the facts mentioned above, it is assumed that preparation of nanoparticles from aromatic derivatives of chitosan can enhance cellular permeability of peptides and proteins.

In this study, we investigated the preparation and optimization of insulin nanoparticles via the Polyelectrolyte complexation (PEC) method composed of three derivatives of chitosan including methylated *N*-(4-*N*,*N*-dimethylaminobenzyl) chitosan, methylated *N*-(4-pyridinyl) chitosan, and methylated *N*-(benzyl) chitosan designated as (aminobenzyl) chitosan, (pyridinyl) chitosan, and (benzyl) chitosan nanoparticles, respectively, as aromatic derivatives. D-optimal response surface methodology has been used for optimization of chitosan-based nanoparticles prepared by PEC and also for determination of the effects of pH of polymer solution, concentration ratio of polymer to insulin, and polymer type on physicochemical properties of nanoparticles including size, zeta potential, polydispersity index (PdI), and entrapment efficiency (EE%).

MATERIALS AND METHODS

Materials

Low molecular weight chitosan (viscosity, 1% (*w*/*v*) solution in acetic acid, 22 mPa s) was obtained from Primex (Iceland). 4-*N*,*N*-dimethylbenzaldehyde, 4-pyridin carbaldehyde, 4-benzaldehyde, *N*-methyl pyrolidone, sodium iodide, iodomethane, triethylamine, sodium hydroxide, and sodium chloride were purchased from Merck (Darmstadt, Germany). Sodium borohydride was provided from Aldrich (UK). Insulin was obtained from Exir Pharmaceutical (Lorestan, Iran). Dialysing tube with a molecular cutoff of 12,000 Da (D0405) was obtained from Sigma. Analytical-grade Lichrosolv® acetonitrile was obtained from Merck (Darmstadt, Germany). All other chemicals were of pharmaceutical grade and used as received.

Synthesis and Characterization of Aromatic Derivatives of Chitosan

Synthesis of N-(4-N,N-dimethylaminobenzyl) Chitosan, N-(4-pyridinyl) Chitosan and N-(benzyl) Chitosan

The chemical structures of the desired aromatic derivatives are shown in Fig. 1. The derivatives were synthesized by modified Schiff base reaction method (24). Chitosan (4 g) was dissolved in 1% acetic acid (100 ml), and then for the reduction of viscosity, the solution was diluted with 100 ml of methanol. The pH of the solution was adjusted to 5.2 by adding 1 N NaOH. The appropriate amount of related aldehyde was added to the solution and stirred for 12 h at room temperature. The amount and type of added aldehydes are summarized in Table I. After formation of appropriate imine, the double bond of the compounds were reduced by freshly prepared gaseous hydrogen prepared by gradual addition of sodium borohydride as the powder to the solution and keeping the solution to be stirred for 8 h at ambient temperature. Then, derivatives were precipitated from the solution by adding 1 N NaOH and adjusting the pH to 9.0. The precipitates were then washed with methanol twice, dissolved in 1% acetic acid and dialyzed for 3 days against distilled water using dialyzing tube. The desired compounds were then precipitated using 1 N NaOH. The precipitates were transferred to a vacuum dryer and stayed overnight for complete drying ascertained by Karl Fischer technique.

Synthesis of Methylated Aromatic Derivatives

Methylation process was accomplished according to previous reports with minor modifications (17). Compounds prepared in the previous section (2 g) was completely dissolved in 70 ml of *N*-methyl pyrolidone under gentle

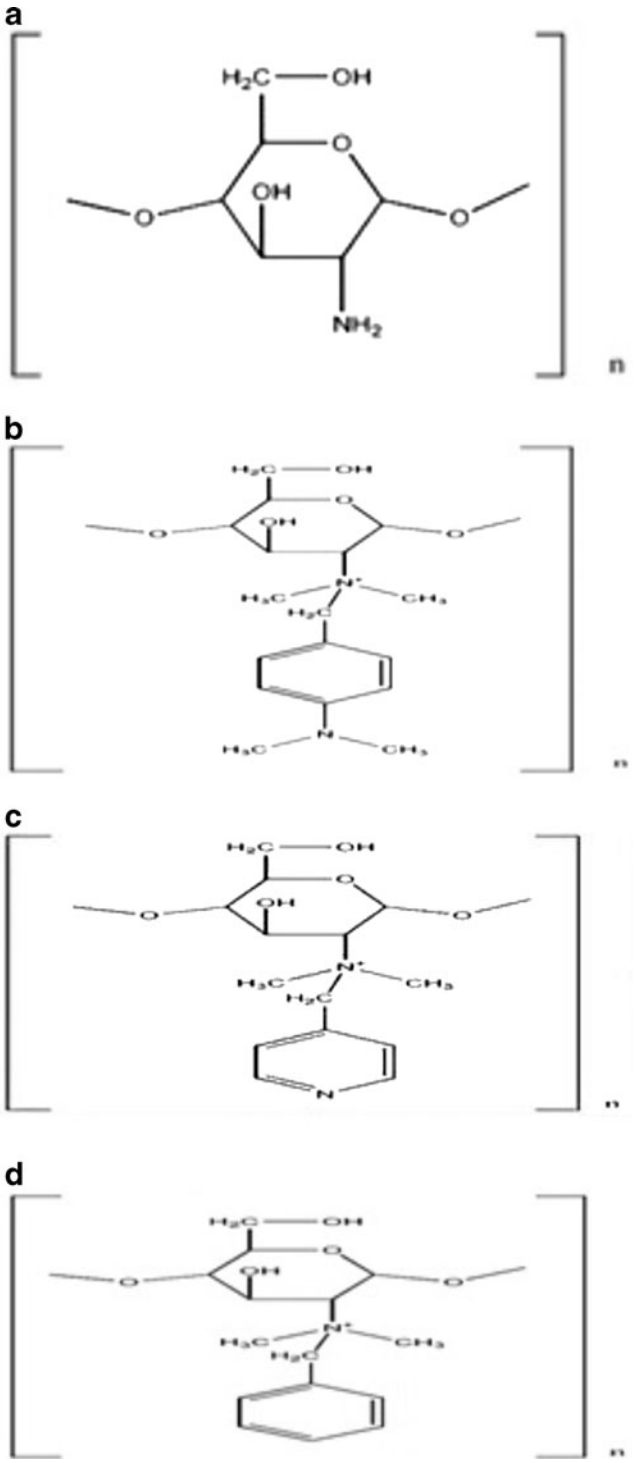

Fig. 1. Chemical structure of **a** chitosan; **b** methylated *N*-(4-*N*,*N*-dimethylaminobenzyl) chitosan; **c** methylated *N*-(4-pyridinyl) chitosan, and **d** methylated *N*-(benzyl) chitosan

magnetic stirring at 50°C. Sodium iodides (1 g), either 3 ml of 42% triethylamine or 5 ml of 1 N NaOH, were then added to the solution. Twelve milliliters of methyl iodide was gradually added in three equal portions over a 3-h period, and the solution was refluxed at 50°C for 12 h. The solution was then transferred to a dialyzing tube and dialyzed against distilled water for 3 days as the previous step. The appropriate compound was precipitated by adding 300 ml of acetone. The obtained derivatives were dissolved in NaCl solution (5%, *w*/*v*) and stirred for 1 h at ambient temperature for exchange of I^- with Cl^-. Then the chloride salt of the desired compounds was then precipitated. The precipitates were transferred to a vacuum dryer and held overnight for complete drying. The quaternized derivatives were characterized by ^{1}H-NMR. D_2O has been used as the solvent for ^{1}H-NMR spectroscopy. Degree of substitution and degree of quaternization were also determined from integrated data obtained from ^{1}H-NMR spectra.

Determination of the Molecular Weight of Derivatives by Gel Permeation Chromatography

Molecular weight of chitosan and the aromatic derivatives were determined using Knauer® Gel permeation chromatography system equipped with PL aquagel OH-MIXED-M 8 μm, 300*7.5 mm column and Knauer® differential refractive index detector. The mobile phase consisted of sodium acetate/acetic acid buffer adjusted to pH of 4.5. The flow rate was kept constant at 1 ml/min. The chromatograms were acquired and integrated by Chromgate® software compatible with Knauer® chromatographic systems.

Preparation of Nanoparticles

Insulin nanoparticles composed of methylated (aminobenzyl), methylated (pyridinyl), and methylated (benzyl) chitosan were prepared by previously reported PEC method (28,29). By this method, nanostructures were prepared due to electrostatic interaction between positively charged polymer and negatively charged insulin. Briefly, 5 ml of insulin (1 mg/ml) with adjusted pH value of 8.0 was added dropwise to the equal volume of polymer solution with appropriate concentration and pH, under 500 rpm magnetic stirring. Previously, both solutions were filtered through 0.22-μm pore size filter. For better electrostatic interaction, the freshly prepared nanocomplexes were kept stirred for further 20 min. After incubation, final pH of nanosuspension was measured. Nanoparticles were obtained by centrifugation of the freshly prepared opalescent colloidal suspension at 15,000 rpm for 30 min at 4°C. Supernatant was separated and collected for further analysis, and nanoparticles were re-suspended in distilled water. Optimization of nanoparticles was performed by D-optimal response surface methodology that will be further discussed in the next section and ultimately, optimized nanoparticles were lyophilized while sucrose 5% (*w*/*v*) was used as lyoprotectant.

Characterization of Nanoparticles

Determination of Size and Zeta Potential of the Particles

Mean diameter and zeta potential of prepared particles were determined by photon correlation spectroscopy (PCS) and laser Doppler anemometry, respectively, using a Zetasizer 3000HS (Malvern Instruments, Malvern, UK). Zeta potential of synthesized derivatives in free soluble form were measured by dissolving chitosan and quaternized derivatives

Table I. Characteristics of Chitosan and Synthesized Derivatives

Polymer	Appropriate aldehyde	Amount of aldehyde	DS (%)	DQ-Ch (%)	DQ-Ar (%)	Recovery	Mw (kg/mol)	Zeta potential (mean±SD)
Methylated (aminobenzyl) chitosan	4-*N*,*N*-dimethylbenzaldehyde	1.3 g	37%	46%	17%	83%	138	56.1±1.68
Methylated (pyridynyl) chitosan	4-Pyridin carbaldehyde	2 ml	42%	43%	4%	71%	140	49.7±2.27
Methylated (benzyl) chitosan	4-Benzaldehyde	3.6 ml	34%	52%	–	78%	138	36.7±1.42
Chitosan	–	–	–	–	–	–	142	23±1.21

DS degrees of substitution, *DQ* degree of quaternization

in aqueous media, and the pH was adjusted to a value of 4.0 using 0.5% (*v*/*v*) acetic acid. Concentration of all solutions was kept constant to be as 1 mg/ml. The results are summarized in Table I. Nanoparticles were diluted at 1:10 ratio by freshly prepared purified water that was previously passed through 0.22-μm filter. All the measurements were performed on triplicate.

Determination of EE% of the Particles

EE% was determined indirectly by subtracting the total amount of insulin used for preparation of particles and amount of non-encapsulated insulin present in the supernatant. The calculations were based on Eq. 1 and the appropriate entrapment efficiency was reported as percent. All freshly prepared nanoparticle samples were centrifuged at 15,000 rpm for 30 min at 4°C, and the supernatant was analyzed for determination of non-encapsulated insulin by HPLC (n=3). Fifty microliters of the samples was injected to Agilent® 1260 infinity equipped with 1260 Quat pump VL, 1260 ALS auto sampler, and 1260 DAD VL detector that was set at 214 nm. MZ® analytical Perfect Sil Target® ODS −3 (125*4.6 mm, 5 μm) column was used for chromatography. The data were acquired using Agilent Chemsation ® software. Mobile phase was consisted of acetonitrile/0.1% trifluroacetic acid (30:70), and the analysis was performed at ambient temperature, as previous report (30). Before injection of the samples, all criteria for method validation include accuracy, precision, linearity, LOD, and LOQ were checked according to ICH guidelines. The method proven to be linear over the wide range of 10 ng/ml to 2 μg/ml. The calculated within-day and between-day precision and accuracy were correlated to the ICH guidelines.

$$\text{EE\%} = [(\text{total amount of insulin} - \text{non} - \text{encapsulated insulin})/\text{total amount of insulin}] * 100 \quad (1)$$

Determination of the Morphology of the Particles

Lyophilized particles were re-suspended in freshly prepared distilled water and related size and shapes were investigated by transmission electron microscopy (TEM), using a CEM 902A (Zeiss, Oberkochen, Germany). In this study, TEM technique was preferred over scanning electron microscopy (SEM) because the effect of re-suspension of lyophilized nanoparticles in aqueous media on morphology of particles can be observed by TEM rather than SEM.

Samples for TEM analysis were prepared by placing drops of lyophilized and re-dispersed nanoparticles on carbon-coated TEM copper grids. The mixtures were allowed to dry for 5 min. The size of NPs was determined by direct observation.

Experimental Design Studies

Studies related to development of drug delivery systems are being performed by changing one variable at a time while other variables have constant values. This so-called change-only-one-separate-factor-at-the-time approach requires lots of experiments and therefore, is time and cost consuming. On the other hand, since the interaction effect between independent variables (factor) will not be discussed, the real well-optimized formulation is unreachable. In order to overcome these problems, design-of-experiment approach (DoE) has been evolved and studied in pharmaceutical issues (31). Screening and optimization by response surface methodology (RSM) are considered as the two major application of DoE in pharmaceutical sciences. Although central composite and Box–Behnken designs are the most studied techniques in RSM, computer-generated D-optimal design is also used in certain conditions. In this study, D-optimal response surface methodology was specifically selected because the effect of a three-leveled categorical variable (polymer type) should be investigated in physicochemical properties of insulin nanoparticles.

Quantitative independent variables (factors) including pH of polymer solution (X_1) and concentration ratio of polymer/insulin (X_2) were defined in appropriate ranges identified by preliminary studies. Polymer type (X_3) was a categorical factor that has been studied in three levels. The ranges and levels of defined factors are indicated in Table II. Dependent variables (responses) were particle size (Y_1), zeta potential (Y_2), PdI (Y_3), and EE% (Y_4).

Design-Expert® software (V. 7.0.0, Stat-Ease, Inc., Minneapolis, USA) has been used for mathematical modeling and evaluation of the responses. Based on this software, performing a total of 20 runs was required to

Table II. Variables Used in D-optimal Response Surface Design

Independent variables (factors)		Levels		
		−1		+1
Numeric factors	Polymer pH (X_1)	3.0		6.5
	Concentration ratio of polymer/insulin (X_2)	0.5		2.0
Categorical factor	Polymer type (X_3)	A Methylated *N*-(4-*N*,*N*-dimethylaminobenzyl) chitosan	B Methylated N-(4-pyridin) chitosan	C Methylated *N*-(benzyl) chitosan
Dependent variables (responses)		Constrains		
Y_1=size (nm)		Minimize		
Y_2=zeta potential (mV)		$20<Y_2<30$		
Y_3=PdI		Minimize		
Y_4=EE%		Maximize		

EE% entrapment efficiency

develop the appropriate models. Finally, the developed models were explained by second-order polynomial functions as follows:

$$Y_{A,B,C} = \beta_0 + \beta_1 X_1 + \beta_2 X_2 + \beta_{11} X_1^2 + \beta_{22} X_2^2 + \beta_{12} X_1 X_2$$

Where:

$Y_{A,\,B,\,C}$ Predicted responses for methylated (aminobenzyl), methylated (pyridinyl), and methylated (benzyl) chitosan, respectively, as types of investigated polymers
β_0 Intercept
β_1 and β_2 Linear coefficients
β_{11} and β_{22} Square coefficients
β_{12} Interaction coefficient
And

X_1 and X_2 Independent quantitative variables

In vitro Insulin Release Studies

In vitro release of insulin from optimized, experimentally designed nanoparticles was determined at 37±2°C in phosphate buffer (pH=6.8) regarded as simulated intestinal fluid (SIF) under gentle stirring. Suitable amount of lyophilized powder equivalent to 200 mg of insulin that provides sink condition was placed into 80 ml of preheated phosphate buffer (pH=6.8), and the dispersion was incubated at 37±2°C under gentle magnetic stirring (100 rpm). At predetermined times, 1 ml of supernatant release medium were collected and replaced by freshly prepared buffer. The individual samples were centrifuged at 20,000 rpm for 30 min and the amount of insulin was determined by HPLC as mentioned previously. All the experiments were performed in triplicate.

RESULTS

Synthesis and Characterization of Aromatic Derivatives of Chitosan

The ^{1}H-NMR spectra of synthesized quaternized aromatic derivatives have been shown in Fig. 2. In Fig. 2a, sharp peaks at 2.4 and 2.7 ppm represent methyl protons of (−N (CH_3)–) and $(-N^+(CH_3)_2-)$, respectively, related to aliphatic amine of methylated (aminobenzyl) chitosan, indicating formation of quaternized derivative. Sharp peaks at 3.4 and 3.6 ppm indicate methyl protons of $(-N(CH_3)_2)$ and $(-N^+(CH_3)_3)$, respectively, belong to aromatic amine that attached to the benzyl ring. In Fig. 2b, peaks at 2.8 and 3.2 ppm are related to protons of methyl groups of (−N

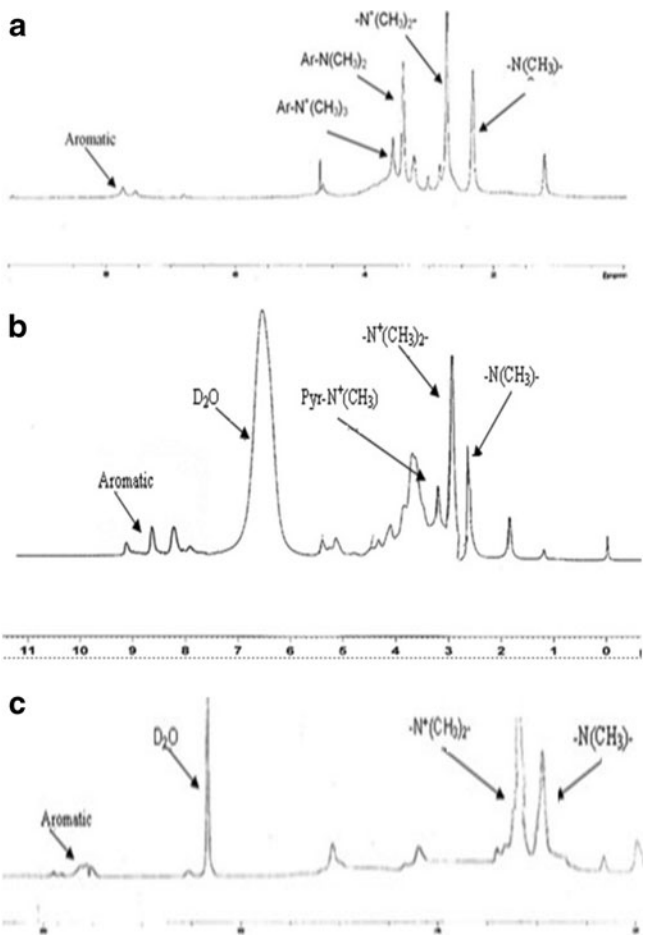

Fig. 2. ^{1}H-NNMR spectra of **a** methylated *N*-(4-*N*,*N*-dimethylaminobenzyl), **b** methylated *N*-(4-pyridinyl) chitosan, and **c** methylated *N*-(benzyl) chitosan

(CH_3)–) and ($-N^+(CH_3)_2$–), respectively related to aliphatic amine of methylated (pyridinyl) chitosan. Small peak at 4.1 indicates quaternization of aromatic amino group. As observed in Fig. 2b and Table I, the low degree of quaternization on amino group of pyridinyl ring was observed. This was due to inlocalised protons of aromatic amino group in the result of conjugation with pyridinyl aromatic ring. In Fig. 2c, peaks at 2.9 and 3.2 ppm indicate protons of (−N (CH_3)–) and ($-N^+(CH_3)_2$–), respectively related to aliphatic amine of methylated (benzyl) chitosan, No other dominant peak was observed in the related spectrum. As shown in Fig. 2, peaks between 7 and 8 ppm are related to protons of proper aromatic ring and indicate formation of aromatic derivatives. Degrees of aromatic substitution, degree of quaternization for both alyphatic and aromatic amines, and also percentage of recovery are summarized in Table I.

Gel permeation chromatography was performed for molecular weight determination of synthesized derivatives. Methylation with NaOH caused a reduction in molecular weight, due to alkaline depolymerization of chitosan as previously reported (32). Depolymerization was not observed to be significant in the case of triethylamine used instead of NaOH. In this case, as observed in Table I, molecular weight of derivatives showed insignificant reduction compared with chitosan. Therefore, methylation in the presence of triethylamine has been suggested. As indicated in Table I, increasing the zeta potential of free soluble polymers resulted in following order: methylated (aminobenzyl) chitosan>methylated (pyridinyl) chitosan> methylated (benzyl) chitosan>chitosan.

Preparation and Characterization of Nanoparticles

D-optimal experimental design was performed for optimization of nanoparticles. The values of independent variables and the related experimental data in 20 suggested formulations based on D-optimal design have been summarized in Table III.

Final pH of freshly prepared nanosuspensions were fall in the range of 5.6 to 7.2. As quaternized chitosan derivatives used in this study, no sign of precipitation was observed at pH of 7.2 and soluble PECs were formed in this pH range.

Size of Particles

Particles with mean diameter ranging from 207±16.71 to 1,385±3.21 nm have been obtained in various D-optimal suggested runs as shown in Table III. It can be observed that all the main factors (*i.e.*, pH of polymer solution, concentration ratio, and polymer type) have influenced the size of nanostructures. 3-D response surface plot of size variation due to changes in independent variables has been shown on Fig. 3a. As shown in Table III and shown in Fig. 3a, at constant concentration ratio, size of particles were increased by increasing the pH from 3.0 to 6.5. As shown in Fig. 3a, this phenomenon was observed in the whole studied range of concentration ratio. While pH was varied between 3.0 and 6.5 at constant concentration ratio of 0.5, size of particles were experienced to change from 207±16.71 to 864±32.38 nm (formulation no. 4 and 5), 241±15.24 to 852±27.46 nm (formulation no. 14 and 16), and 314±35.94 to 671± 27.50 nm (formulation no. 15 and 2) for methylated(aminobenzyl), methylated (pyridinyl), and methylated (benzyl) chitosan nanoparticles, respectively (Table III).

At constant pH, size of particles has slightly increased by increasing the concentration ratio in predetermined range indicated in Fig. 3a. As shown in the figure, when the concentration ratio was varied between 0.5 and 2.0 at constant pH value of 3.0, size of particles were varied from 207±16.71 to 382±40.67 nm (formulation no. 4 and 9) and 314±35.94 to 534±28.32 nm (formulation no. 15 and 3) for

Table III. D-optimal Experimental Design

Formulation no.	Independent variables (factors)			Dependent variables (responses)			
	X_1	X_2	X_3	Y_1 (nm) (mean±SD)	Y_2 (mV) (mean±SD)	Y_3 (mean±SD)	Y_4 (%) (mean±SD)
1	6.5	2.00	C	1,042±36.98	21.8±2.05	0.934±0.06	18.7±2.28
2	6.5	0.50	C	671±27.50	14.2±1.37	0.767±0.09	12.4±5.41
3	3.0	2.00	C	534±28.32	25.2±1.15	0.541±0.07	45.2±3.26
4	3.0	0.50	A	207±16.71	35.7±1.40	0.131±0.04	62.7±1.82
5	6.5	0.50	A	864±32.38	21.4±2.75	0.663±0.04	17.3±2.15
6	4.7	0.50	B	376±41.66	21±1.81	0.391±0.03	65.8±4.37
7	6.5	1.25	B	956±32.11	22.6±1.53	0.682±0.05	58.3±3.54
8	4.7	1.25	C	347±12.80	20.5±1.72	0.474±0.08	74.5±1.16
9	3.0	2.00	A	382±40.67	45.1±2.64	0.337±0.06	76.9±2.83
10	6.5	2.00	A	1,385±53.21	27.8±0.90	0.782±0.08	33.1±2.04
11	4.7	2.00	B	621±22.86	28.5±1.35	0.594±0.04	85.7±1.90
12	3.0	1.25	B	343±11.00	33.1±1.76	0.373±0.01	70.3±3.72
13	4.7	0.88	A	267±23.90	34.6±1.82	0.286±0.03	79.4±4.11
14	3.0	0.50	B	241±15.24	33.2±2.67	0.257±0.06	58.6±2.73
15	3.0	0.50	C	314±35.94	23.6±0.55	0.363±0.05	31.5±3.95
16	6.5	0.50	B	852±27.46	15.8±1.06	0.645±0.03	33.6±2.24
17	4.7	2.00	B	593±38.21	27.2±2.18	0.577±0.04	92.7±1.61
18	6.5	2.00	A	1,352±37.07	26.1±1.93	0.740±0.04	38.4±4.32
19	3.0	2.00	A	391±18.54	46.8±3.19	0.376±0.02	71.2±3.15
20	6.5	2.00	C	925±39.55	20.5±0.61	1	20.3±1.94

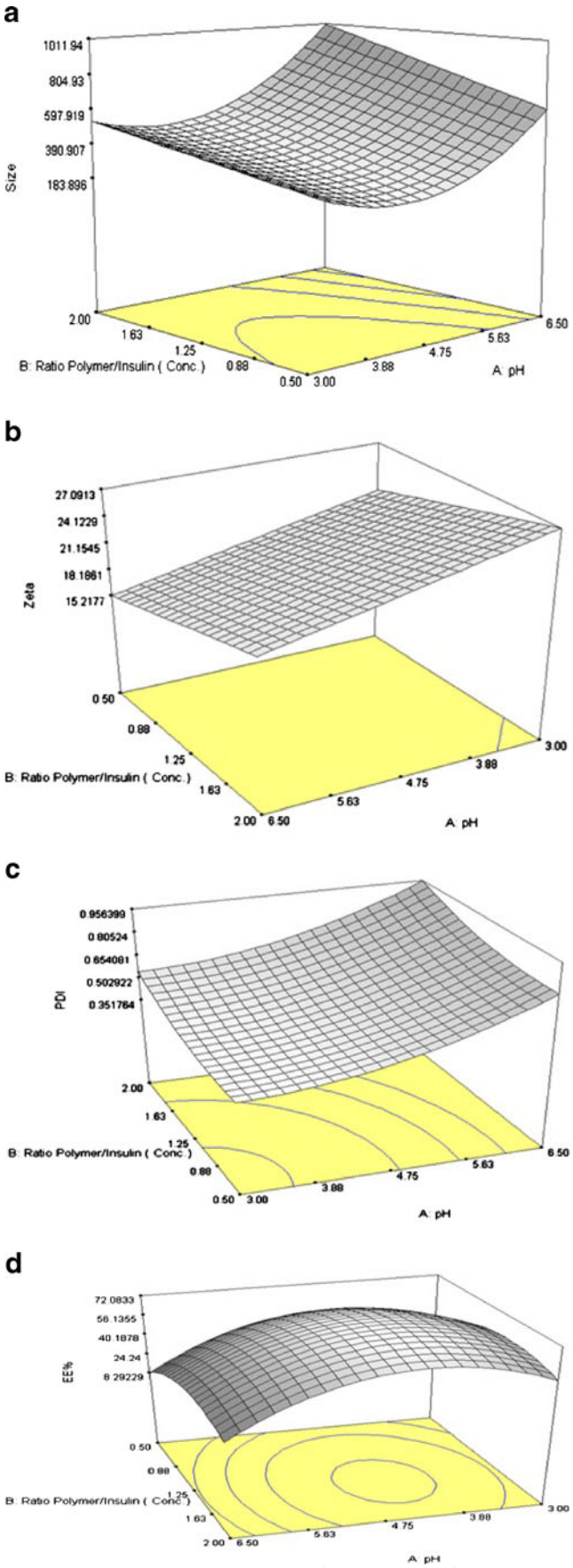

Fig. 3. 3-D response surface plots for **a** size, **b** zeta potential, **c** PdI, and **d** EE% of nanoparticles prepared from methylated *N*-(benzyl) chitosan

methylated (aminobenzyl) and methylated (benzyl) chitosan nanoparticles, respectively (Table III). The same trend was observed for methylated (pyridinyl) chitosan nanoparticles. Previous studies have shown in insulin pH of 8.0, size of particles will be increased by increasing the polymer concentration (33).

Statistical analysis, performed by Design-Expert® based on D-optimal response surface methodology was applied to establish the best significant fitted model for prediction of size of particles ($P<0.01$). The characteristics of fitted model have been provided in Table IV. Regression analysis of variance for data showed that the linear coefficients of all independent factors, the squared coefficient of X_1 and interaction coefficients of $X_1 \cdot X_2$ and $X_2 \cdot X_3$ were significant ($P<0.05$). The coefficients of significant variables have shown in Eqs. 2 to 4 as follows:

$$Y_{1A} = 1,158.04 - 605.02 * (X_1) + 30.02 * (X_2) + 84.15 * (X_1)^2 + 36.74 * (X_1) \cdot (X_2) \quad (2)$$

$$Y_{1B} = 1,408.79 - 656.81 * (X_1) + 30.02 * (X_2) + 84.15 * (X_1)^2 + 36.74 * (X_1) \cdot (X_2) \quad (3)$$

$$Y_{1C} = 1,691.37 - 734.30 * (X_1) + 30.02 * (X_2) + 84.15 * (X_1)^2 + 36.74 * (X_1) \cdot (X_2) \quad (4)$$

Where:

$Y_{1A,\ 1B,\ 1C}$	Predicted responses for sizes of nanoparticles prepared from methylated (aminobenzyl), methylated (pyridinyl), and methylated (benzyl) chitosan
X_1	pH value of polymer solutions
X_2	Concentration ratio of polymer/insulin
$X_1 \cdot X_2$	Interaction coefficient of pH value and concentration ratio

Zeta Potential

Zeta potential of particles determines the stability of colloidal nanosuspensions (34). Generally, stability of nanostructures was higher at high zeta potential values due to great electrostatic repulsion force between particles. On the other hand, surface charge can influence the cell cytotoxicity of particles. Cytotoxicity studies of nanoparticles have been shown that particles with high positive zeta potential values may significantly reduce the cell viability (35). Therefore, zeta potential maybe considered as one of the main physicochemical properties of particles that should be studied. As shown in Table II, constrain for optimization of zeta potential has been considered as the range of 20 to 30 mV. Particles with zeta potential value higher than 30 mV may pose cytotoxic properties on epithelial cells. On the other hand, particles

Table IV. Characteristics of Models Fitted to Responses

Dependent variables (responses)	Best-fitted model	R^2	Adj R^2	Pred R^2	Adeq–precision	Lack of fit
Size (Y_1)	Quadratic	0.9812	0.9675	0.9394	26.27	Insignificant ($P>0.1$)
Zeta potential (Y_2)	2 FI	0.9581	0.9387	0.8909	23.21	Insignificant ($P>0.05$)
PdI (Y_3)	Quadratic	0.9796	0.9702	0.9442	32.93	Insignificant ($P>0.1$)
EE% (Y_4)	Quadratic	0.9790	0.9637	0.9208	24.42	Insignificant ($P>0.1$)

EE% entrapment efficiency

with zeta potential values lower than 20 mV tend to be aggregated and will not be stable. 3-D response surface plot of zeta potential of particles is shown in Fig. 3b.

As depicted in Table III, zeta potential of obtained particles varied from 14.2±1.37 to 46.8±3.19 mV. As shown in Fig. 3b, zeta potential of particles was at the maximum level when the pH of polymer solution was low (pH=3.0) and decrease with increasing pH. As will be discussed, the observed decrease in zeta potential may be due to reduction in protonation degree of free amino groups.

Concentration ratio of polymer/insulin (as one the main factors) had significant effect on surface charge. It is shown that with increasing the concentration ratio, zeta potential of particles increased due to increasing the total mass of positively charged polymer.

At constant concentration ratio and pH values, zeta potential of particles prepared from different polymer types were maximum for methylated (amino benzyl) chitosan and minimum for methylated (benzyl) chitosan, in accordance with data obtained from zeta potential determination of free polymers presented in Table I. The specification of best-fitted model has been indicated in Table IV. Regression analysis of variance for data, showed that the linear coefficients of all independent factors and interaction coefficient of $(X_1)\cdot(X_3)$ were significant ($P<0.05$) and should be considered in the model. The coefficients of significant variables have shown in Eqs. 5 to 7 as follows:

$$Y_{2A} = 52.1 - 4.86 * (X_1) + 3.60 * (X_2) \quad (5)$$

$$Y_{2B} = 41.29 - 4.15 * (X_1) + 3.60 * (X_2) \quad (6)$$

$$Y_{2C} = 25.41 - 1.89 * (X_1) + 3.60 * (X_2) \quad (7)$$

Where:

$Y_{2A,\ 2B,\ 2C}$ Predicted responses for sizes of nanoparticles prepared from methylated (aminobenzyl), methylated (pyridinyl), and methylated (benzyl) chitosan
X_1 pH value of polymer solutions
X_2 Concentration ratio of polymer/insulin

Polydispersity Index

PdI, an index represents the homogeneity of nanodispersions, is ranged from 0 to 1. Homogeneity of nanosuspension becomes higher as the PdI approach to zero (36). 3-D response surface plot of observed PdI has been shown in Fig. 3c.

It can be observed from Fig. 3c that at constant concentration ratio, PdI was increased by increasing of the pH of polymer solution. This was experienced for all three types of polymers. Increasing pH from 3.0 to 4.7 had caused slightly elevation in PdI while in pH range of 4.7 to 6.5, small changes in pH could cause a sharp increase in PdI.

In the case of methylated (pyridinyl) chitosan nanoparticles at concentration ratio of 0.5, PdI increased from 0.257±0.06 to 0.391±0.03 (formulation no. 14 and 6) in consequence to pH increasing from 3.0 to 4.7. Further increases in polymer pH resulted a sharp increase in PdI in a manner that it was reported to be 0.645±0.03 (formulation no. 16) in the upper limit of pH range (*i.e.*, pH=6.5) at the constant concentration ratio, stated above. Same trend was observed for methylated (aminobenzyl) and methylated (benzyl) chitosan nanoparticles.

As shown in Fig. 3c, at constant pH, PdI increased linearly in the result of increasing the polymer/insulin concentration ratio. At polymer pH value of 3.0, PdI was increased from 0.131±0.04 to 0.337±0.04 (formulation no. 4 and 9) and 0.363±0.05 to 0.541±0.07 (formulation no. 15 and 3) for methylated (aminobenzyl) and methylated (benzyl) chitosan nanoparticles respectively, in accordance with increasing the concentration ratio from 0.5 to 2.0 (Table III). In the case of methylated (pyridinyl) chitosan, PdI was increased from 0.257±0.06 to 0.373±0.01 (formulation no. 14 and 12) when the concentration ratio of polymer/insulin increased from 0.5 to 1.25 (Table III).

It was observed that the polymer type has significant effect on PdI of nanoparticles. At constant pH and concentration ratio, the maximum PdI was observed for methylated (benzyl) chitosan nanoparticles while the minimum belongs to methylated (aminobenzyl) chitosan (data have not been shown).

The experimental data were fitted to a significant statistical model ($P<0.01$) that has been indicated in Table IV. Regression analysis of variance for data showed that linear coefficients of all independent factors and square coefficient of X_1 and X_2 were significant ($P<0.05$) and should be considered in the model. No interaction effect was found significant in this model ($P>0.1$). The coefficients of significant variables have shown in Eqs. 8 to 10 as follows:

$$Y_{3A} = 0.461 - 0.174 * (X_1) - 0.139 * (X_2) + 0.030(X_1)^2 + 0.106 * (X_2)^2 \quad (8)$$

$$Y_{3B} = 0.562 - 0.174 * (X_1) - 0.139 * (X_2) + 0.030 * (X_1)^2 + 0.106 * (X_2)^2 \quad (9)$$

$$Y_{3C} = 0.644 - 0.174 * (X_1) - 0.139 * (X_2) + 0.030 * (X_1)^2 + 0.106 * (X_2)^2 \quad (10)$$

Where:

$Y_{3A,\ 3B,\ 3C}$	Predicted responses for sizes of nanoparticles prepared from methylated (aminobenzyl), methylated (pyridinyl), and methylated (benzyl) chitosan
X_1	pH value of polymer solutions
X_2	Concentration ratio of polymer/insulin

Entrapment Efficiency

Calculated EE% of insulin nanoparticles was varied between wide range of 18.7%±2.28% to 85.7±1.90% depending on pH of polymer solution, concentration ratio and polymer type. 3-D response surface plot of calculated EE% is shown in Fig. 3d. In contrast to ionic gelation method that hydrophobic interaction and H-bounding are considered as dominant mechanisms by which the drug is entrapped into particles (28,37), in PEC method, it is obvious that drug entrapment is occur due to electrostatic interactions.

A second-order significant effect of concentration ratio on EE% has been observed. As shown in Fig. 3d, at constant pH, by increasing the concentration ratio from 0.5 to 1.25, EE% was increased until the maximum has been obtained. Further increases in concentration ratio from 1.25 to 2.0, cause decrease in EE% of particles. Jinkapattankit *et al.* (38) have explained that increasing the concentration of polymer may cause rigidity of polymer and consequently decrease of EE%.

As presented in Table III, in the case of methylated (pyridinyl) chitosan nanoparticles, at constant concentration ratio of 0.5, the studied EE% was raised from 58.6± 2.73% to 65.8±4.37% (formulation no. 14 and 6) by increasing the pH from 3.0 to 4.7. By further increasing of pH, EE% was sharply decreased and reached to the value of 33.6±2.24% in pH value of 6.5 (formulation no. 16). The same behavior was observed for nanoparticles prepared by other polymers.

Nanoparticles prepared from methylated (pyridinyl) chitosan shown the maximum EE% while minimum entrapment has been observed for nanoparticles prepared by methylated (benzyl) chitosan (data have not been not shown).

The regression analysis of variance for data, showed that the linear coefficients of all independent factors, square coefficient of all quantitative factors and also the interaction coefficient of $(X_1)\cdot(X_3)$ were significant ($P<0.05$) and should be considered in the model. The coefficients of significant variables have shown in Eqs. 11 to 13 as follows:

$$Y_{4A} = -114.85 + 76.00 * (X_1) + 72.66 * (X_2) - 9.22 * (X_1)^2 - 25.22 * (X_2)^2 \quad (11)$$

$$Y_{4B} = -140.68 + 82.34 * (X_1) + 72.66 * (X_2) - 9.22 * (X_1)^2 - 25.22 * (X_2)^2 \quad (12)$$

$$Y_{4C} = -157.02 + 80.76 * (X_1) + 72.66 * (X_2) - 9.22 * (X_1)^2 - 25.22 * (X_2)^2 \quad (13)$$

Where:

$Y_{4A,\ 4B,\ 4C}$	Predicted responses for sizes of nanoparticles prepared from methylated (aminobenzyl), methylated (pyridinyl), and methylated (benzyl) chitosan
X_1	pH value of polymer solutions
X_2	Concentration ratio of polymer/insulin

Optimization and Model Validation

The optimization of physicochemical properties of nanoparticles was performed based on statistical analysis of experimentally obtained data. D-optimal response surface method was used for optimization. Table V indicates the optimized and predicted conditions for preparation of nanoparticles. For model validation and determination of prediction error, the nanoparticles prepared experimentally and characterized ($n=5$). The observed responses followed by predicated error value were indicated in Table VI. As shown in the Table, the calculated prediction errors were below 5% for all conditions. This represents the significance, adequacy, and predictability of models.

Morphology of Nanoparticles

Images obtained from TEM have been shown in Fig. 4. As illustrated in this figure, the morphology of particles prepared from methylated (aminobenzyl), methylated (pyridinyl), and methylated (benzyl) chitosan are identical. TEM images have shown larger particle size for methylated

Table V. Optimized Independent Variables and Predicted Responses

	Optimized independent variables		Predicted dependent variables (responses)			
Polymer type (X_3)	Polymer pH (X_1)	Concentration ratio (X_2)	Y_1=size (nm)	Y_2=zeta potential (mV)	Y_3=PdI	Y_4=EE%
A	5.0	0.61	365	30	0.312	69.4
B	3.9	1.02	305	28.7	0.319	88.2
C	4.0	1.09	292	21.8	0.415	67.8

EE% entrapment efficiency

Table VI. Observed Responses and Prediction Errors for Model Validation

	Dependent variables (responses)							
	Size (nm)		Zeta potential (mV)		PdI		EE%	
X_3	Observed response (mean±SD)	Prediction error (%)	Observed response (mean±SD)	Prediction error (%)	Observed response (mean±SD)	Prediction error (%)	Observed response (mean±SD)	Prediction error (%)
A	346±35.3	−5.04	28.5±1.98	−4.73	0.305±0.05	−2.24	70.3±3.27	1.35
B	318±58.8	4.26	27.7±2.15	−3.27	0.333±0.04	4.51	84.5±5.31	−4.14
C	289±24.7	−1.02	22.2±2.96	1.83	0.437±0.05	5.39	69.2±4.72	2.09

EE% entrapment efficiency

(aminobenzyl) nanoparticles compared with other derivatives, in accordance with observed values obtained by PCS method for experimentally optimized nanoparticles. The data for PCS analysis are shown in Table VI as observed responses for size. The particles were morphologically round to oval shape with a smooth surface. No sign of aggregation has been observed for the nanosuspensions.

In vitro Release Study

In vitro release of insulin from optimized nanoparticles in phosphate buffer at pH value of 6.8 representing SIF medium according to USP was studied and the results have been illustrated in Fig. 5. As shown in this figure, in nanoparticles prepared from methylated (aminobenzyl), methylated (pyridinyl) and methylated (benzyl) chitosan, the mean percentage of insulin release were observed to be 36.1%, 25.3%, and 19.9%, respectively, within 30 min. This result represent low burst release in all nanoparticles, indicating suitable interaction between insulin and polymer. It has been shown previously, that nanoparticulate systems prepared by PEC method can pose relatively small burst release (39).

According to Fig. 5, the cumulative percentage of insulin release from nanoparticles were 47.1%, 38%, and 68.7% for methylated (aminobenzyl), methylated (pyridinyl), and methylated (benzyl) chitosan, respectively, within 300 min under studied conditions stated above.

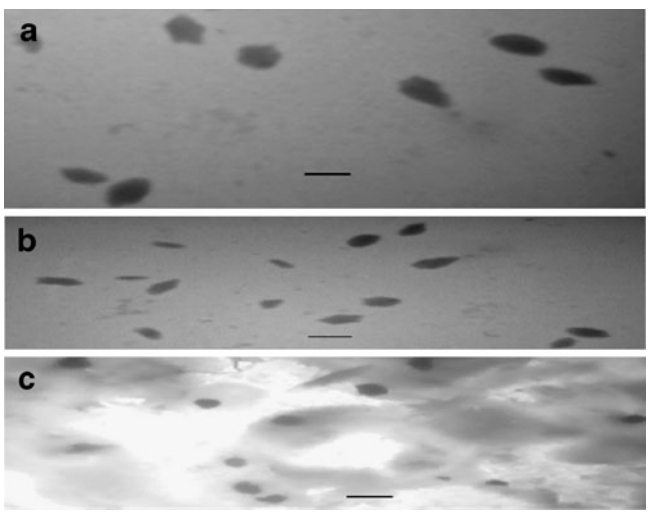

Fig. 4. TEM images of nanoparticles composed of **a** methylated *N*-(4-*N*,*N*-dimethylaminobenzyl) chitosan, **b** methylated *N*-(4-pyridinyl) chitosan, and **c** methylated *N*-(benzyl) chitosan. The *scale bar in the right corner of each image* represents 350 nm

DISCUSSION

Polymeric nanoparticles regarded as solid colloidal carriers are composed of synthetic, semi-synthetic or natural polymers incorporating the active drug and ranging from 10 to 500 nm in diameter.

Various studies have investigated the use of polymers such as poly-lactide-*co*-glycolide (40,41), chitosan (42,43), albumin (44), and so on in peptide delivery.

Chitosan can enhance the cellular absorption by two mechanism: (a) mucoadhesion, that is caused by the interaction between positively charged polymer and negatively charged sialic acid groups in mucin and (b) reversible opening of tight junctions due to redistribution of F-actin caused by interaction between polymer which pose positively and negatively charged sites on cell surfaces. (45,46).

In recent years, ionic gelation and PEC method have been widely investigated as suitable techniques for preparation of nanoparticles from sensitive molecules like peptide and proteins. These methods eliminate the requirement for sonication and organic solvent during fabrication, therefore, minimize possible damage to peptide. Sadeghi *et al.* (29) have shown that PEC method can produce insulin nanoparticles

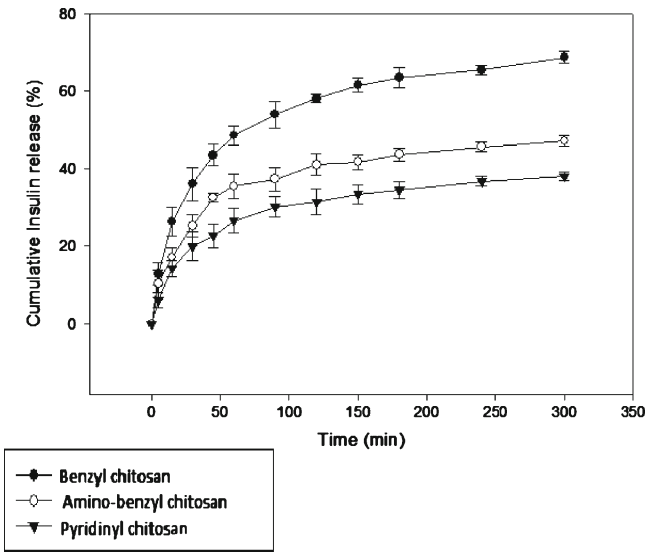

Fig. 5. Cumulative insulin release profile from nanoparticles in phosphate buffer (pH=6.8)

with higher loading efficiency and also higher zeta potential compared with ionic gelation method. On the other hand, Jintapattanakit *et al*. (38) have produced smaller particles with lower PdI by PEC method compared with ionic gelation. They have shown that self assembled insulin nanoparticles produced by PEC, pose higher stability in SIF and also more protected from enzymatic degradation in the presence of serine protease and trypsin in comparison with TPP/insulin nanoparticles produced via ionic gelation (38).

It is obvious that quaternized derivatives pose higher zeta potential than chitosan. Among studied quaternized derivatives, methylated (benzyl) chitosan has shown the lowest zeta potential due to lack of aromatic amino functional group. Since its aromatic amino group involved in conjugation with the aromatic ring, methylated (pyridinyl) chitosan pose lower zeta potential compare with methylated (aminobenzyl) chitosan. This observation is well correlated to literature. Mao *et al*. (33) have reported formation of large particles at higher pH for chitosan nanoparticles manufactured by PEC. Nasti *et al*. (47) also have obtained larger size of insulin nanoparticles prepared by ionic gelation method in high pH values. It is assumed that increase in electrostatic interaction between polymer and insulin in low pHs results in formation of compacted nanoparticles. At lower limit of polymer pH range (*i.e.*, pH=3.0), zeta potential of particles become high due to protonation of free, non-quaternized amines (either aliphatic or aromatic) that exist in the backbone structure of the polymers. The high electrostatic repulsion force between particles due to high positive surface charge makes particles to be more compacted. Therefore, as observed and previously mentioned, particles become smaller in lower pH values compared with higher pH values. The great zeta potential of particles in low pH values makes particles to be stable and non-aggregated and provides greater electrostatic interaction between polymer and drug. At upper limit of range for polymer pH (*i.e.*, pH=6.5), degree of protonation of free amino functional groups will be significantly reduced, causes low zeta potential of particles and consequently, increase the tendency of aggregation and producing larger particles. Therefore, size of particles increased in higher pH values.

As shown in chemical structure of derivatives in Fig. 1, monomers of both methylated *N*-(4-*N*,*N*-dimethylaminobenzyl) chitosan and methylated *N*-(4-pyridin) chitosan have one extra aromatic amino functional group which are partially quaternized compare with methylated *N*-(benzyl) chitosan that has no aromatic amine. It is assumed that zeta potential of nanoparticles prepared by methylated (aminobenzyl) and methylated (pyridinyl) derivatives are more pH dependent than methylated (benzyl) chitosan due presence of one extra amino functional group in the structure of former polymers.

Entrapment efficiency was low in polymer pH of 3.0 that relates to the final pH value of 5.3 in the system after complexation and preparation of particles due to decreased negative charge density of insulin. The electrostatic interaction between chitosan derivatives and insulin is shown to be increased by increasing the pH until the polymer pH reaches to the proper value of 4.7. At this pH, the positive charge density of the polymer structure is at favorable level to interact with negatively charged drug. Consequently, entrapment efficiency will be high in pH value of 4.7. In this polymer pH value, the final pH of the system was observed to be near isoelectric pH of insulin (*i.e.*, pH=6.1). It was reported that polymers can entrap proteins at pH around isoelectric point (48) . By further increase in pH, the surface charge of the polymers decreased sharply and interaction between polymer and insulin will be interrupted due to lack of proper positive charge on the polymer surface. This can explain the sharp decrease in EE% in consequence of increasing the pH from 4.7 to 6.5.

The fast *in vitro* release of insulin from methylated (benzyl) chitosan nanoparticles can be justified by considering the fact that this polymer poses the lowest zeta potential among the other polymers used for preparation of nanoparticles and negatively charged insulin cannot efficiently interact with the polymer. As methylated (aminobenzyl) chitosan is expected to be higher soluble in aqueous media compared with methylated (pyridinyl) chitosan due to lack of inlocalized amino group which is present in methylated (pyridinyl) chitosan, higher release rate can be expected from methylated(aminobenzyl) chitosan nanoparticles compare with methylated (pyridinyl) chitosan.

CONCLUSIONS

In this study, three quaternized aromatic derivatives of chitosan including methylated *N*-(4-*N*,*N*-dimethylaminobenzyl) chitosan, methylated *N*-(4-pyridinyl) chitosan, and methylated *N*-(benzyl) chitosan have been synthesized used for preparation of insulin nanoparticles by PEC method. Prepared nanoparticles were optimized using D-optimal response surface experimental design methodology. The effect of formulation variables including pH of polymer solution, concentration ratio of polymer to insulin, and polymer type on nanoparticles' characteristics including size, zeta, PdI, and entrapment efficiency was also studied. Optimized nanoparticles were characterized as small in size, low in PdI, suitable positive zeta potential that may promote epithelial permeability of particles and also high entrapment efficiency. Morphological study of particles revealed formation of non-aggregated, uniformly sized, to oval shape particles with smooth surfaces. Insulin *in vitro* release study was performed on nanoparticles, and the results have shown little burst release demonstrating well-established interaction between polymer and insulin.

ACKNOWLEDGMENTS

This study was made possible by financial supports from Deputy of Research, Tehran University of Medical Sciences and the National Committee of Nanotechnology.

REFERENCES

1. Tan ML, Choong PFM, Dass CR. Recent developments in liposomes, microparticles and nanoparticlesfor protein and peptide drug delivery. Peptides. 2010;31:184–93.
2. Moghimi SM, Szebeni J. Stealth liposomes and long circulating nanoparticles: critical issues in pharmacokinetics, opsonization and protein-binding properties. Prog Lipid Res. 2003;42:463–78.

3. Soppimath KS, Aminabhavi TM, Kulkarni AR, Rudzinski WE. Biodegradable polymeric nanoparticles as drug delivery devices. J Control Release. 2001;70:1–20.
4. Reiss CP, Neufeld RJ, Ribeiro AJ, Veiga F. Nanoencapsulation II. Biomedical applications and current status of peptide and protein nanoparticulate delivery systems. Nanomedicine. 2006;2:53–65.
5. McClean S, Prosser E, Meehan E, O'Malley D, Clarke N, Ramtoola Z, *et al*. Binding and uptake of biodegradable poly-d, l-lactide microand nanoparticles in intestinal epithelia. Eur J Pharm Sci. 1998;6:153–63.
6. Reiss CP, Neufeld RJ, Ribeiro AJ, Veiga F, Nanoencapsulation I. Methods for preparation of drug-loaded polymeric nanoparticles. Nanomedicine. 2006;2:8–12.
7. El-Sayed A, Remawi MA, Qinna N, Farouk A, Bedwan A. Formulation and characterization of an oily-based system for oral delivery of insulin. Eur J Pharm Biopharm. 2009;73:269–79.
8. Surendiran A, Sandhiya S, Pradhan SC, Adithan C. Novel applications of nanotechnology in medicine. Indian J Med Res. 2009;130:689–701.
9. Bhumkar DR, Joshi HM, Sastry M, Pokarkar VB. Chitosan reduced gold nanoparticles as novel carriers for transmucosal delivery of insulin. Pharm Res. 2007;24:1415–26.
10. Slomkowski S, Gosecki M. Progress in nanoparticulate systems for peptide, proteins and nucleic acid drug delivery. Curr Pharm Biotechnol. 2011; (in press)
11. Tiwari AK, Gajbhiye V, Sharma R, Jain NK. Carrier mediated protein and peptide stabilization. Drug Deliv. 2010;17:605–16.
12. Ramesan RM, Sharma CP. Challenges and advances in nanoparticles-based oral insulin delivery. Expert Rev Med Devices. 2009;6:665–76.
13. Lubben IM, Verhoef JC, Borchard G, Junginger HE. Chitosan and its derivatives in mucosal drug and vaccine delivery. Eur J Pharm Sci. 2001;14:201–7.
14. Artursson P, Lindmark T, Davis SS, Illum L. Effect of chitosan on the permeability of monolayers of intestinal epithelial cells (Caco-2 cells). Pharm Res. 1994;11:1358–61.
15. Sadeghi AMM, Dorkoosh FA, Avadi MR, Weinhold M, Bayat A, Delie F, *et al*. Permeation enhancer effect of chitosan and chitosanderivatives: comparison of formulations as soluble polymers and nanoparticulate systems on insulin absorption in Caco-2 cells. Eur J Pharm Biopharm. 2008;70:270–8.
16. Ubaidulla U, Kishan Khar R, Ahmed FJ, Panda AK. Development and *in-vivo* evaluation of insulin-loaded chitosan phthalate microspheres for oral delivery. J Pharm Pharm. 2007;59:1345–51.
17. Sieval AB, Thanou M, Kotze AF, Verhoef JC, Brusse J, Junginger HE. Preparation and NMR characterization of highly substituted IV-trimethyl chitosan chloride. Carbiohydr Polymer. 1998;36:157–65.
18. Avadi MR, Zohuriaan-mehr MJ, Younessi P, Amini M, Rafiee-Tehrani M, Shafiee A. Optimized synthesis and characterization of *N*-triethyl chitosan. J Bioact Compat Polym. 2003;18:469–79.
19. Bayat A, Sadeghi AMM, Avadi MR, Amini M, Majlesi R, Junginger HE, *et al*. Synthesis of *N*,*N*-dimethyl *N*-ethyl chitosan as a carrier for oral delivery of peptide drugs. J Bioact Compat Polym. 2006;21:433–44.
20. Kafedjiiski K, Hoffer M, Werle M, Bernkop-Schnurch A. Improved synthesis and *in vitro* characterization of chitosan-thioethylamidine conjugate. Biomaterials. 2006;27:127–35.
21. Yoo HS, Lee JE, Chung H, Kwon IC, Jeong SY. Self-assembled nanoparticles containing hydrophobically modified glycol chitosan for gene delivery. J Control Release. 2005;103:235–43.
22. Sandri G, Rossi S, Bonferonji MC, Ferrari F, Zambito Y, Di Colo G, *et al*. Buccal penetration enhancement properties of *N*-trimethyl chitosan: Influence of quaternization degree on absorption of a high molecular weight molecule. Int J Pharm. 2005;297:146–55.
23. Sandri G, Bonferoni MC, Rossi S, Ferrari F, Gibin S, Zambito Y, *et al*. Nanoparticles based on *N*-trimethylchitosan: evaluationof absorption properties using *in vitro* (Caco-2 cells) and *ex vivo* (excised rat jejunum) models. Eur J Pharm Biopharm. 2007;65:68–77.
24. Rojanarata T, Petchsangsai M, Opanasopit P, Ngawhirunpat T, Uracha Ruktanonchai U, Sajomsang W, *et al*. Methylated *N*-(4-*N*,*N*-dimethylaminobenzyl) chitosan for novel effective gene carriers. Eur J Pharm Biopharm. 2008;70:207–14.
25. Kowapradit J, Opanasopit P, Ngawhiranpat T, Apirakaramwong A, Rojanarata T, Ruktanonchai U, *et al*. Methylated *N*-(4-*N*,*N*-dimethylaminobenzyl) chitosan, a novel chitosan derivative, enhances paracellular permeability across intestinal epithelial cells(Caco-2). AAPS PharmSci Tech. 2008;9:1143–52.
26. Kowapradit J, Opanasopit P, Ngawhiranpat T, Rojanarata T, Sajomsang W. Structure–activity relationships of methylated *N*-aryl chitosan derivatives for enhancing paracellular permeability across Caco-2 cells. Carbohydr Polym. 2011;83:430–7.
27. Jung T, Kamm W, Breitenbach A, Kaiserling E, Xiao JX, Kissel T. Biodegradable nanoparticles for oral delivery of peptides: is there a role for polymers to affect mucosal uptake? Eur J Pharm Biopharm. 2000;50:147–60.
28. Mao S, Germershaus O, Fischer D, Linn T, Schnepf R, Kissel T. Uptake and transport of PEG-graft-trimethyl-chitosan copolymer–insulin nanocomplexes by epithelial cells. Pharm Res. 2005;22:2058–68.
29. Sadeghi AMM, Dorkoosh FA, Avadi MR, Saadat P, Rafiee-Tehrani M, Junginger HE. Preparation, characterization and antibacterial activities of chitosan, *N*-trimethyl chitosan (TMC) and *N*-diethylmethyl chitosan (DEMC) nanoparticles loaded with insulin using both the ionotropic gelation and polyelectrolyte complexation methods. Int J Pharm. 2008;355:299–306.
30. Sarmento B, Ribeiro A, Veiga F, Sampaio P, Neufeld R, Ferreira D. Alginate/chitosan nanoparticles are effective for oral insulin delivery. Pharm Res. 2007;24:2198–206.
31. Wold S, Sjostrom M, Eriksson L. PLS-regression: a basic tool of chemometrics. Chemom Intell Lab Syst. 2001;58:109–30.
32. Niederhofer A, Müller BW. A method for direct preparation of chitosan with low molecular weight from fungi. Eur J Pharm Biopharm. 2004;57:101–5.
33. Mao S, Bakowsky U, Jintapattankit A, Kiessel T. Self-assembled polyelectrolyte nanocomplexes between chitosan derivatives and insulin. J Pharm Sci. 2006;95:1035–48.
34. Woitiski CB, Veiga F, Ribeiro A, Neufeld R. Design for optimization of nanoparticles integrating biomaterials for orally dosed insulin. Eur J Pharm Biopharm. 2009;73:25–33.
35. Thanou MM, Kotzé AF, Scharringhausen T, Luessen HL, De Boer AG, Verhoef JC, *et al*. Effect of degree of quaternization of N-trimethyl chitosan chloride for enhanced transport of hydrophilic compounds across intestinal caco-2 cell monolayers. J Control Release. 2000;64:15–25.
36. Giannotti MI, Esteban O, Oliva M, García-Parajo MF, Sanz F. pH-responsive polysaccharide-based polyelectrolyte complexes as nanocarriers for lysosomal delivery of therapeutic proteins. Biomacromolecules. 2011;12:2524–33.
37. Nielson L, Khurana R, Coats A, Frokjaer S, Brange J, Vyas S, *et al*. Effect of environmental factors on the kinetic of insulin fibril formation: elucidation of molecular mechanism. Biochemistry. 2001;40:6036–46.
38. Jintapattanakit A, Junyaprasert VB, Mao S, Sitterberg J, Bakowsky U, Kissel T. Peroral delivery of insulin using chitosan derivatives: a comparative study of polyelectrolyte nanocomplexes and nanoparticles. Int J Pharm. 2007;342:240–9.
39. Fresta M, Puglisi G, Giammona G, Cavallaro G, Micali N, Furneri PM. Pefloxacin mesilate and ofloxacin-loaded polyethylcyanoacrylate nanoparticles: characterization of the colloidal drug carrier formulation. J Pharm Sci. 1995;84:895–902.
40. Wada R, Hyon SH, Ikada Y. Lactic acid oligomer microspheres containing hydrophilic drugs. J Pharm Sci. 1989;79:919–24.
41. Uchida T, Yagi A, Oda Y, Nakada Y, Goto S. Instability of bovine insulin in poly (lactide-co-glycolide) (PLGA) microspheres. Chem Pharm Bull. 1996;44:235–6.
42. Werele M, Takeuchi H, Bernkop-Schnurch A. Modified chitosans for oral drug delivery. J Pharm Sci. 2009;98:1643–56.
43. Dicolo G, Zambito Y, Zanico C. Polymeric enhancers of mucosal epithelia permeability: synthesis, transepithelial penetration-enhancing properties, mechanism of action, safety issues. J Pharm Sci. 2008;97:1652–80.

44. Reiss CP, Viega FJ, Riberio J, Neufeld R, Damge C. Nanoparticulate biopolymers deliver insulin orally eliciting pharmacological response. J Pharm Sci. 2008;97:5290–305.
45. McEwan G, Jepson M, Hirst B, Simmons N. Polycationinduced enhancement of epithelial paracellular permeability is independent of tight junctional characteristics. Biochim Biophys Acta. 1993;1148:51–60.
46. Lin YH, Mi FL, Chen CT, Chang WC, Peng SF, Liang HF, *et al*. Preparation and characterization of nanoparticles shelled with chitosan for oral insulin delivery. Biomacromolecules. 2007;8:146–52.
47. Nasti A, Zaki NM, De Leonardis P, Ungphaiboon S, Sansongsak P, Rimoli MG, *et al*. Chitosan/TPP and chitosan/TPP-hyaluronic acid nanoparticles: systematic optimisation of the preparative process and preliminary biological evaluation. Pharm Res. 2009;26:1918–30.
48. Muzzarelli RA, Barontini G, Rocchetti R. Immobilized enzymes on chitosan columns: alpha-chymotrypsin and acid phosphatase. Biotech Bioeng. 1976;18:1445–54.